Inverse Analysis of Multiple Indentation Unloading Curves for Thin Film Young's Modulus Evaluation

Joris Prou, Kikuo Kishimoto, Kazuaki Inaba, Andrei Constantinescu

Inverse Analysis of Multiple Indentation Unloading Curves for Thin Film Young's Modulus Evaluation

Joris PROU*, Kikuo KISHIMOTO*, Kazuaki INABA* and Andrei CONSTANTINESCU**

* *Tokyo Institute of Technology, Graduate School of Sciences and Engineering, Department of Mechanical Sciences and Engineering, Tokyo, Japan*

** *École Polytechnique, Laboratoire de Mécanique des Solides (CNRS UMR 7649), Palaiseau, France*

The Oliver and Pharr method is the prevailing process for thin films Young's modulus evaluation. Introduced initially for homogeneous materials, this method does not account for the substrate and can consequently lead to significant error, especially at large indentation depths. We suggest here possible methods to improve the accuracy by making use of inverse analysis and finite element computations of the one layer elastic indentation problem.

1 INTRODUCTION

The identification of Young's moduli from the indentation test is essentially based on the ideas proposed in 1992 by Oliver and Pharr[1)]. Under the assumptions of an elastic unloading and small strains, Oliver and Pharr used Sneddon's closed form solution for the indentation of an elastic half-space with a flat punch to evaluate the Young's modulus of bulk materials. This method applied to homogeneous materials usually gives identified values in a good agreement with the specimen Young's modulus.

Although introduced in the case of bulk materials and consequently does not account for the substrate, the Oliver and Pharr method remains the most widely used method for thin films Young's modulus characterization. To prevent errors related to the substrate, a generally admitted rule is to limit indentation depth to 10% of the film thickness. Nevertheless, the method demonstrates limitations in precision for large mismatch between film and substrate properties and for ultra-thin films where the control of indentation depth is close to the limitations of the measurement.

An improvement of the method in the case of thin-films which takes both film and substrate into account has recently been proposed by Li and Vlassak[2)]. They suggested to replace the Sneddon's solution for the half space in the method with Yu et al.s'[3)] semi-analytical solution of a layered elastic half-space. The Yu's solution is fast to obtain by numerical methods, as it is the iterative solution of an integral equation, however the procedure is complex to implement.

In this work, we suggest some extensions to the preceding methods by Oliver and Pharr, Li and Vlassak for estimation of thin films Young's modulus from indentation experiments. The idea is also based on the unloading curve combined with an inverse analysis of the data, the difference lies in replacing the closed form solution of the methods with a finite element computation to solve the layered indentation problem. As such the method is closed to the formulation of Li and Vlassak but offers the advantages of the finite element method. Within the advantages we can cite the high modularity and the easy implementation in commercially available codes and an important extension of the underlying assumptions of the analysis: graded materials, multiple layers, friction, etc..

This paper starts by a brief description of the Oliver and Pharr method as well as the improvement by Li and Vlassak in order to set the proposed method back in context. The developed methods are presented and finally applied to numerical experiments to discuss their legitimacy and further possible improvements.

2 METHODS: STATE OF THE ART

2.1 Oliver and Pharr Method

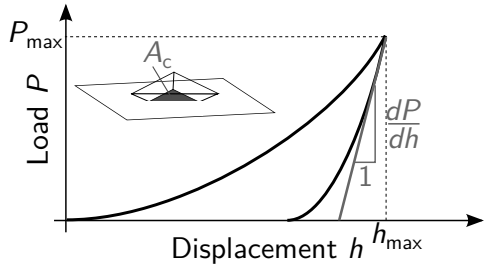

Fig. 1 Typical indentation load-displacement curve

Introduced in 1992 by Oliver and Pharr for homogeneous elastic-plastic materials, this method is by far the most widely used for evaluating elastic moduli from continuous indentation test and is generally directly incorporated in the indentation apparatus. The Young's modulus can then be obtained directly from the unloading part of the indentation load-displacement curve (Fig. 1). This method takes advantage of the assumption that the early stage of the unloading can be considered as elastic, and can thus utilize Sneddon closed form relation[4] between the load and displacement of the indenter derived for axisymmetric indenter on an indented linear elastic half-space. It makes use of the following semi-empirical relation first established by Loubet *et al.*[5]:

$$E^* = \frac{1}{2}\sqrt{\frac{\pi}{A_c}}\frac{dP}{dh}\bigg|_{h_{max}} \tag{1}$$

with $\frac{dP}{dh}\Big|_{h_{max}}$ the contact stiffness at the initial stage of the unload, A_c the projected contact area at maximum load and E^* the effective modulus defined in eq. (2).

$$\frac{1}{E^*} = \frac{1-\nu^2}{E} + \frac{1-\nu_{ind}^2}{E_{ind}} \tag{2}$$

where E, ν are respectively the Young's modulus and Poisson's ratio of the indented sample and E_{ind}, ν_{ind} those of the indenter.

The difficulty faced with the direct use of this relation comes from the inaccurate evaluation the contact surface. Indeed, due to the elastic recovery and the possibility of pile-up or sink-in (see Fig. 2), the contact surface at maximum load is different from the residual imprint after unloading. If the contact depth h_c and the shape of the indenter tip are known, then Eq. (3) becomes for the case of the three sided pyramidal Berkovitch indenter:

$$E^* = \frac{1}{2h_c}\sqrt{\frac{\pi}{24.5}}\frac{dP}{dh}\bigg|_{h_{max}} \tag{3}$$

To identify this contact depth, Oliver and Pharr showed first that the unloading curve is well described by a power law of the following form:

$$P = A(h - h_f)^m \tag{4}$$

where h_f is the depth of the residual imprint, A and m are some constants depending on the material and the indenter, which are obtained by fitting the above relation with the unloading curve. This allowing a precise calculation of contact stiffness $\left.\frac{dP}{dh}\right|_{h_{max}}$.

Furthermore, they suggested that the contact depth should be estimated by subtracting the elastic deflection to the maximum indentation depth:

$$h_c = h_{max} - \epsilon \frac{P_{max}}{\left.\frac{dP}{dh}\right|_{h_{max}}} \tag{5}$$

where ϵ is a geometrical factor depending solely on the indenter shape, $\epsilon = 0.72$ for a Berkovitch indenter.

This method applied to bulk materials shows that in most cases a good estimation can be achieved with less than 10% of error[6]. However, it should be noticed that this procedure does not take into account the pile-up effect.

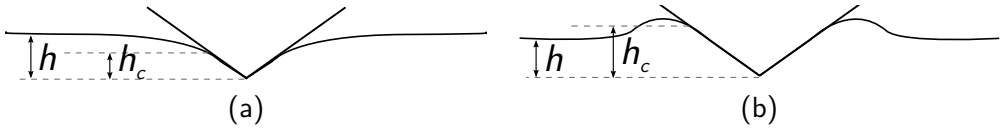

Fig. 2 Contact depth: (a) sink-in - (b) pile-up

Although first introduced for bulk materials, this method can still be applied for thin films but under certain restrictions. In order to avoid the substrate influence on the load displacement curve, a general practical rule is to consider that for an indentation with a maximum penetration of 10% of the coating thickness. Though, it was pointed out in[7,8] that in case of super-hard coatings this rule is insufficient to obtain precise results. Moreover, it should be noted that, for very thin films (few dozens of nanometers) performing an indentation at 10% of the thickness is limited by the apparatus precision, and indenter size problems.

2.2 Li and Vlassak Impoved Method

To account for the substrate effect in the elastic modulus evaluation, Li and Vlassak introduced recently[2] a related method based here on Yu's solution for a layered elastic half-space that can be obtained numerically. Assuming the elastic parameters, this offers almost instantaneously a relation between the contact area and contact stiffness of layered elastic material, and allows a generalization of the Oliver and Pharr method.

The hypotheses followed in this approach are:

- small deformations in order to use Yu's elastic solution
- modification of the elastic film thickness by introducing an effective thickness to integrate the local thinning effect of the elasto-plastic film below the indenter as a consequence of the plastic flow

- contact radius in the elastic-plastic indentation estimated in a similar way as in the Oliver and Pharr method, but a correction factor is introduced to represent the substrate influence. The factor depends on the elastic properties of the film and substrate as well as the thinning parameter described above.

The reduced modulus can then be retrieved by inverse analysis minimizing the discrepancy in the contact radius from Yu's solution and the experimental one. The minimization is performed with respect to the elastic moduli and to the effective film thickness.

Although relying on inverse analysis, a fast computation is ensured considering the fact that the relationship between contact area contact stiffness can be derived from Yu's solution almost instantaneously. This allows also high precision in the computation and this independently of the film thickness / contact radius ratio. However, this method is limited to a single layered material and also by the implementation difficulties to compute Yu's solution.

3 METHODS: PROPOSED EXTENSIONS

We suggest here two different methods aiming at the evaluation of thin films Young's modulus. The idea is essentially based on similar concepts as Oliver-Pharr[1)], and also as Li and Vlassak[2)]. The main assumption is here again:

[C1] *the initial state of the unloading can be considered as elastic*

The contact stiffness for homogeneous materials is well described by Eq. (6), showing a direct relation between contact area and contact stiffness independent of the plastic properties. Therefore, the initial slope of the unloading curve for a elastic-plastic material should match the tangent at the load-displacement curve for an elastic material with the same elastic properties for the same contact area (Fig. 3). This elastic contact stiffness can be obtained from finite element simulation.

$$\frac{1}{E^* A_c}\frac{dP}{dh}\bigg|_{h_{max}} = cst \tag{6}$$

Using a similar reasoning applied for the case of thin film, it can be deduced that the contact stiffness is independent of the plastic properties. Meanwhile, the material in this case does not have to be homogeneous. The contact stiffness is depending not only on the elastic properties of the material and the contact area but also on the deformed geometry if we assume large displacements of large strains during the contact.

If we further assume that

[C2] *the elastic and elastic-plastic deformations geometries are similar*

then the conditions **[C1]** and **[C2]** are fulfilled, an estimation of the contact stiffness dP/dh for a given set of elastic properties and contact area can be obtained from finite element simulations of the elastic layered material indentation.

Compared to Li and Vlassak's method described above, the coupling with finite element allows more flexibility in the indented material model; multiple layers or continuous distribution of the elastic parameters can be considered. These methods also contrast with usual inverse analyses applied to the indentation experiment, which require first to infer a plastic behavior model for the materials in the simulation in order to fit experimental data, and second to perform the identification not only for

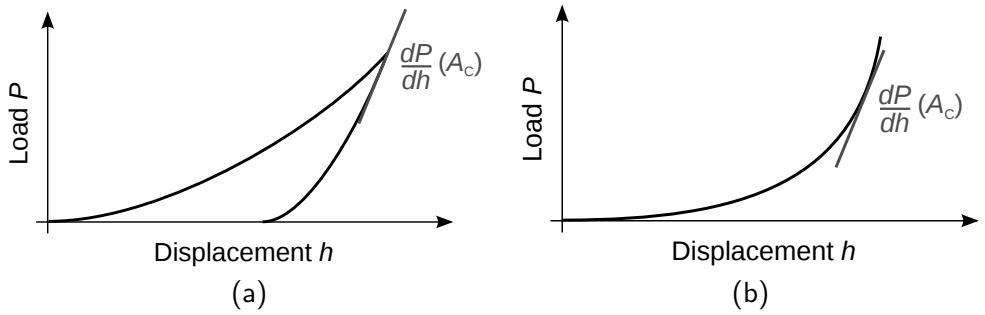

Fig. 3 Correspondence of plastic curve initial unloading slope (a) and tangent to the elastic curve (b) when same contact area A_c

elastic parameters but also plastic ones leading to heavier computations and stronger hypotheses. The two proposed methods rely on the same inverse problem approach and the major difference lying in the evaluation of the contact stiffness which will be described in the following sections. In the method guidelines, we propose first to perform n indentations experiments on the elastic-plastic sample for different maximum indentation depths (subsequently different contact areas at maximum load). Then these experimental data are used during an inverse analysis relying on the cost-function $\mathcal{J}$ defined in Eq. (7). $\mathcal{J}$ quantifies the discrepancy between simulated elastic contact stiffness and experimental elastic-plastic contact stiffness

$$\mathcal{J}(E_{film}) = \frac{1}{2}\sum_{k=1}^{n}\left[\left(\frac{dP_{FEM}}{dh}(E_{film}, A_c^k) - \frac{dP_{meas}}{dh}(A_c^k)\right) \Big/ \left(\frac{dP_{meas}}{dh}(A_c^k)\right)\right]^2 \tag{7}$$

where E_{film} denotes the film Young's modulus, dP_{FEM}/dh the tangent at the computed elastic load-displacement curve, A_c^k the contact area at maximum load for the k^{th} plastic indentation experiment, and dP_{meas}/dh the corresponding initial slope at the unloading curve from experimental data.

The minimization of this cost-function $\mathcal{J}$ is performed by a gradient based algorithm (Levenberg-Marquardt). The gradient of $\mathcal{J}$ being required, a fast computation is obtained by implementing a direct differentiation technique[9].

The identification process can then be formalized as follows:

(1) perform n indentation experiments and extract $\frac{dP_{meas}}{dh}(A_c^k)$ and A_c^k for k from 1 to n ;

(2) assume initial value for E_{film} ;

(3) compute $\frac{dP_{FEM}}{dh}(E_{film}, A_c^k)$ for the different A_c^k ;

(4) **if** $\mathcal{J}(E_{film}) \leq$ tolerance
return E_{film} ;
else update E_{film} using Lenvenberg-Marquardt ;
go to step (3) ;

We shall further consider two cases for the step (3) of the algorithm which will be denoted by: nonlinear method and linear elastic method.

3.1 Nonlinear Method

The finite element computation of the contact stiffness dP_{FEM}/dh is performed here for the problem indentation layered elastic material. An iterative procedure is necessary due to the contact conditions

and possible large strains non-linearities. The symmetry of the problem allows to use computations in axisymmetric conditions. Axisymmetric computations can still be used for the Berkovich indenter (three sided pyramid) by introducing an equivalent conical indenter with an effective angle that gives the same ratio between contact depth and contact area. Condition **[C2]** is assumed to be well satisfied if the plastic flow is not too much important during the elastic-plastic indentation.

The computation time is significantly reduced compared to usual inverse analyses, however is still sizeable compared to Vlassak's approach. Another limitation to this method can arise depending on the finite element solver used. Indeed, computational problems may occur at large indentation depths due to the over-distorted mesh at near the vicinity of the indenter tip. In order to overcome these constraints, a method using stronger approximations is outlined in the next section.

3.2 Linear Elastic Method

In the case of indentation of bulk material, the relation between Young's modulus, contact area and contact stiffness is independent of the indenter shape. In the case of thin films, this statement still holds as observed by Vlassak[2)]. From this observation, we propose to use a finite element simulation with the simplified geometries shown in Fig.4 (b) - (d) (flat indenter and conical indenter). The contact stiffness dP_{FEM}/dh can now be obtained from elastic computations with imposed displacement on the contact surface A_c. This approximation can greatly reduce the direct problem computation time and possible mesh problems.

The calculations are limited to small strains and in order to recreate well the indented elastic-plastic material geometry and then satisfy **[C2]**, we make use of the concept of representative thickness introduced by Vlassak, here denoted by h_{rep}. Further study will be necessary for determining the representative thickness h_{ref}, nevertheless as a preliminary study we shall consider two representative thicknesses $h^1_{rep} = h_{film}$ and $h^2_{rep} = h_{film} - (h - h_{cont})$, where h_{film}, h and h_{cont} are respectively the film thickness, the indentation depth and the contact depth (see Fig. 4).

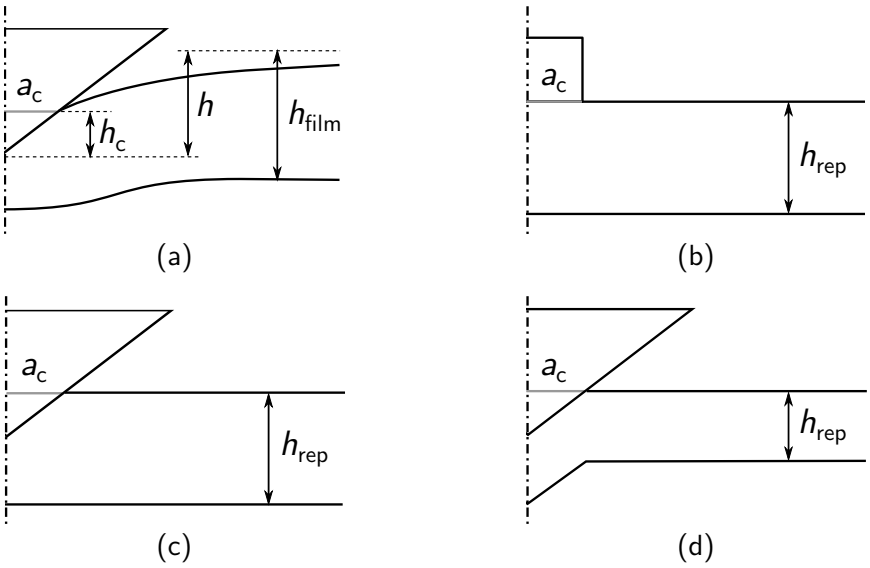

Fig. 4 Scheme of the local deformations at maximum indentation depth (a) and corresponding simplified model for the finite element computation: flat punch model (b), cone model 1 (c) and cone model 2 (d)

4 NUMERICAL RESULTS & DISCUSSIONS

All the finite element computations for simulated load-displacement curves and contact stiffness have been performed using the finite element solver cast3m[10].

4.1 Nonlinear Method

This method was previously investigated numerically[9] for different sets of elastic-prefectly plastic films and substrate. The pseudo-experimental data were obtained from finite element computations for the ratio E_{film}/E_{sub} ranging from 1/4 to 4, and for the ratio $E/\sigma^Y = 1/500$ and 1/50. During the identification data corresponding to a maximum indentation depth of 1/15, 1/10 and 1/5 of the film thickness were simultaneously used. The results were promising and where the film Young's modulus value was generally identified with less than 5% error.

4.2 Linear Elastic Method

To investigate the accuracy of this method, a study is conducted using pseudo-experimental load-displacement curves. These curves are computed from finite element computations of the indentation problem of an elastic-plastic film with kinematic hardening on elastic substrate. The film and substrate properties are given as follows: $E_{film} = 2.5$ GPa, $\nu_{film} = 0.34$, $\sigma^Y_{film} = 69$ MPa, $H_{film} = 234$ MPa, $E_{sub} = 0.25$, 1, 2.5, 6.25 and 25 GPa, $\nu_{sub} = 0.33$. The different values used for the substrate Young's modulus correspond to the ratios $E_{film}/E_{sub} = 1/10$, 2/5, 1, 5/2, 10 and were chosen in order to investigate the effect of the elastic mismatch. The numerical experiments are carried with a conical indenter of effective angle 70.3° representing the Berkovich indenter of semi-angle 65.3°.

For each film substrate combination, simulations are repeated to obtain 10 simulated experimental points corresponding to a maximum indentation depth of 10 to 100 % of the film thickness. However, for the case of compliant film with $E_{film}/E_{sub} = 2/5$ and 1/10, data could be computed only up until 70 and 60 %.

The contact areas are needed as inputs for the inverse analysis and the identification was performed using contact areas estimated following the Oliver and Pharr method and measured from the residual imprints. The identification is carried out for the film Young's modulus only, all the other properties are assumed to be known.

The Young's modulus identification results as well as a comparison with the Oliver and Pharr method for the different ratio of E_{film}/E_{sub} are displayed in Figs. 5 to 8. The identified values are normalized by the film Young's modulus used for the elastic plastic data and are plotted against the normalized indentation depth h/h_{film}. For $h/h_{film} = 0.2$ to 0.9, each point corresponds to identification carried out with data from three consecutive maximum indentation depth and h/h_{film} refers to the mean value of the indentation depth. For $h/h_{film} = 0.1$ and 1.0, represents identification using data respectively at $h/h_{film} = 0.1$, 0.2 and 0.9, 1.0.

Figs. 5 and 6 correspond to the flat model where the contact areas are estimated respectively from the Oliver and Pharr method and the residual imprint. The first result is that the proposed method give more accurate results than the Oliver and Pharr (O&P in the graphs) except for the case $E_{film}/E_{sub} = 1$ with contact area estimated from Oliver and Pharr. As expected the Oliver and Pharr method is influenced by the substrate and as the indentation gets deeper, the identified values get closer to the substrate value leading to large errors. At low indentation depth, the flat punch model approximates well the elastic-plastic deformations and give decent results, but for deep indentations it fails to reproduce the deformations and lead to a loss of accuracy. The identification results

for stiffer substrate when using contact areas from residual imprint are slightly better than the ones estimated from the Oliver and Pharr method. In these cases the substrate is not deforming much and a large plastic flow of the film is induced by the vertical confinement, resulting to a residual imprint area close to the one at maximum load. One can remark that the effect representative thickness is small for stiff substrate. In this case, as the film bears most of the deformations and pile-up will occur. The contact depth will be similar to the indentation depth and as a result $h^1_{rep} \approx h^2_{rep}$. Moreover, since the Young's modulus of the film is lower than the one of the substrate, a small change in the film thickness as a small influence on the contact stiffness.

The estimation results for the simplified cone models are presented in Figs. 7 and 8. Model 1 corresponds to Fig. 4 (c) and model 2 to Fig. 4 (d). For the model 1, the results are similar to the simplified punch model, but for model 2 the accuracy in the estimation suddenly drops for normalized indentation depth around 0.5. This is thought to be consequence of the sharp corner introduce at the interface between film and substrate causing stress concentrations that have a large impact on the computed contact stiffness. Consequently, this accuracy problem might be fixed by introducing smooth edges in the simplified cone model.

The accuracy of the different methods with respect with the indentation depth are shown in Fig. 9. The graphs present a comparison of the maximum indentation depth to obtain an accuracy of 10 and 20 % in the identified values, and are given as a function of the ratio E_{film}/E_{sub}. In order to make a fair comparison with the Oliver and Pharr method, the results for the proposed extensions are given using the Oliver and Pharr contact area estimation and the simplest relative thickness $h^1_{rep} = h_{film}$. The maximum depths are obtained from interpolation and extrapolation of the results in Fig. 5 and 7. In the results, extrapolated values of the maximum depth that were lower than 0 or greater than 1 have been set respectively to 0 and 1.

Fig. 9 shows first that the Oliver and Pharr method using 10 % rule of thumb failed to give a 20 % accuracy for high difference between film and substrate Young's moduli. When the ratio E_{film}/E_{sub} get close to 1, 10 % accuracy could be achieved. Second, using the proposed extensions that accounts for the substrate we could obtain 10 % and 20 % accuracy with maximum indentation depths around 20 % and 30 % of the film thickness independently of the E_{film}/E_{sub} ratio. Nevertheless, the influence of the substrate is still obvious and the simpled geometry model need to be refined. Moreover, in both methods the results are better for compliant films than stiff films. A possible reason is that for stiffer films the substrate bears most of the deformations leading to a real contact area smaller than the one estimated with the Oliver and Pharr method. The identified film Young's modulus is consequently underestimated. Thus, modification for the estimation of the contact area should also be considered to obtain decent identified values at deeper indentation depths.

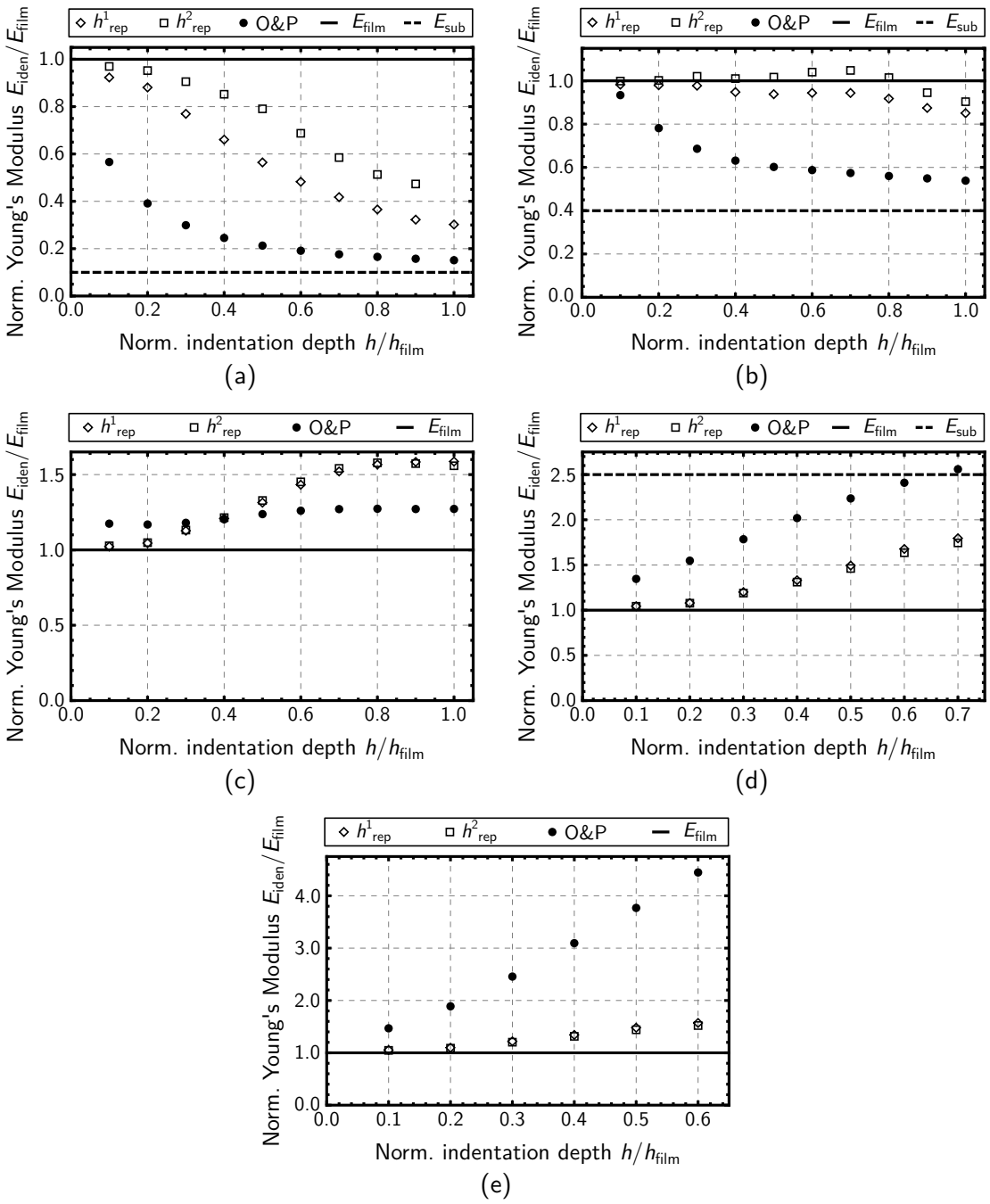

Fig. 5 Identified Young's modulus for the flat punch model using $h_{rep} = h^1_{rep}$ and h^2_{rep}, and contact areas evaluated from the Oliver and Pharr method. A comparison is given with estimated values from the Oliver and Pharr method denoted here by O&P. The results are presented for the following film - substrate combinations: (a) $E_{film}/E_{sub} = 10$, (b) $E_{film}/E_{sub} = 5/2$, (c) $E_{film}/E_{sub} = 1$, (d) $E_{film}/E_{sub} = 2/5$ and (e) $E_{film}/E_{sub} = 1/10$

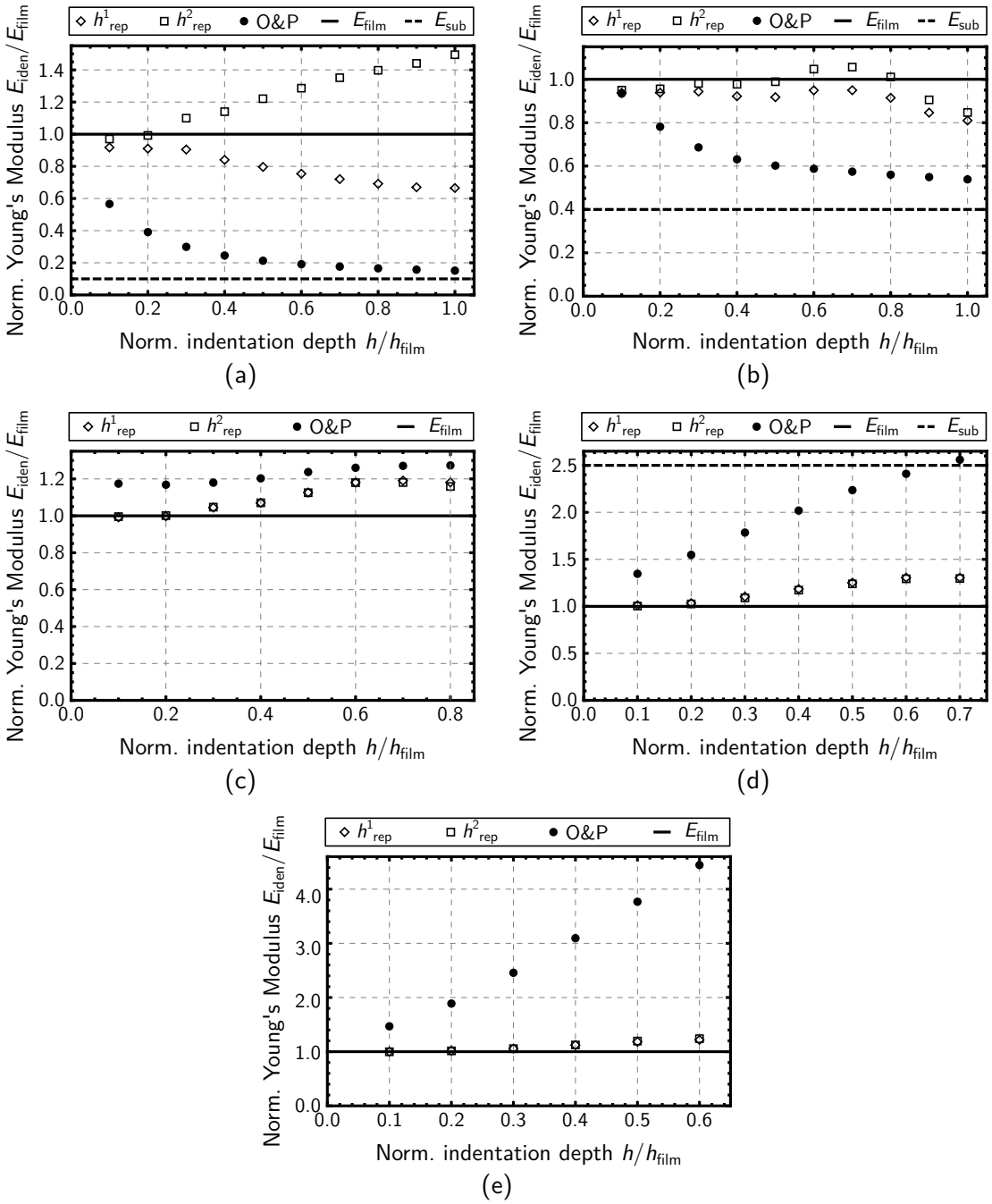

Fig. 6 Identified Young's modulus for the flat punch model using $h_{rep} = h^1_{rep}$ and h^2_{rep}, and contact areas evaluated from the residual imprint. A comparison is given with estimated values from the Oliver and Pharr method denoted here by O&P. The results are presented for the following film - substrate combinations: (a) $E_{film}/E_{sub} = 10$, (b) $E_{film}/E_{sub} = 5/2$, (c) $E_{film}/E_{sub} = 1$, (d) $E_{film}/E_{sub} = 2/5$ and (e) $E_{film}/E_{sub} = 1/10$

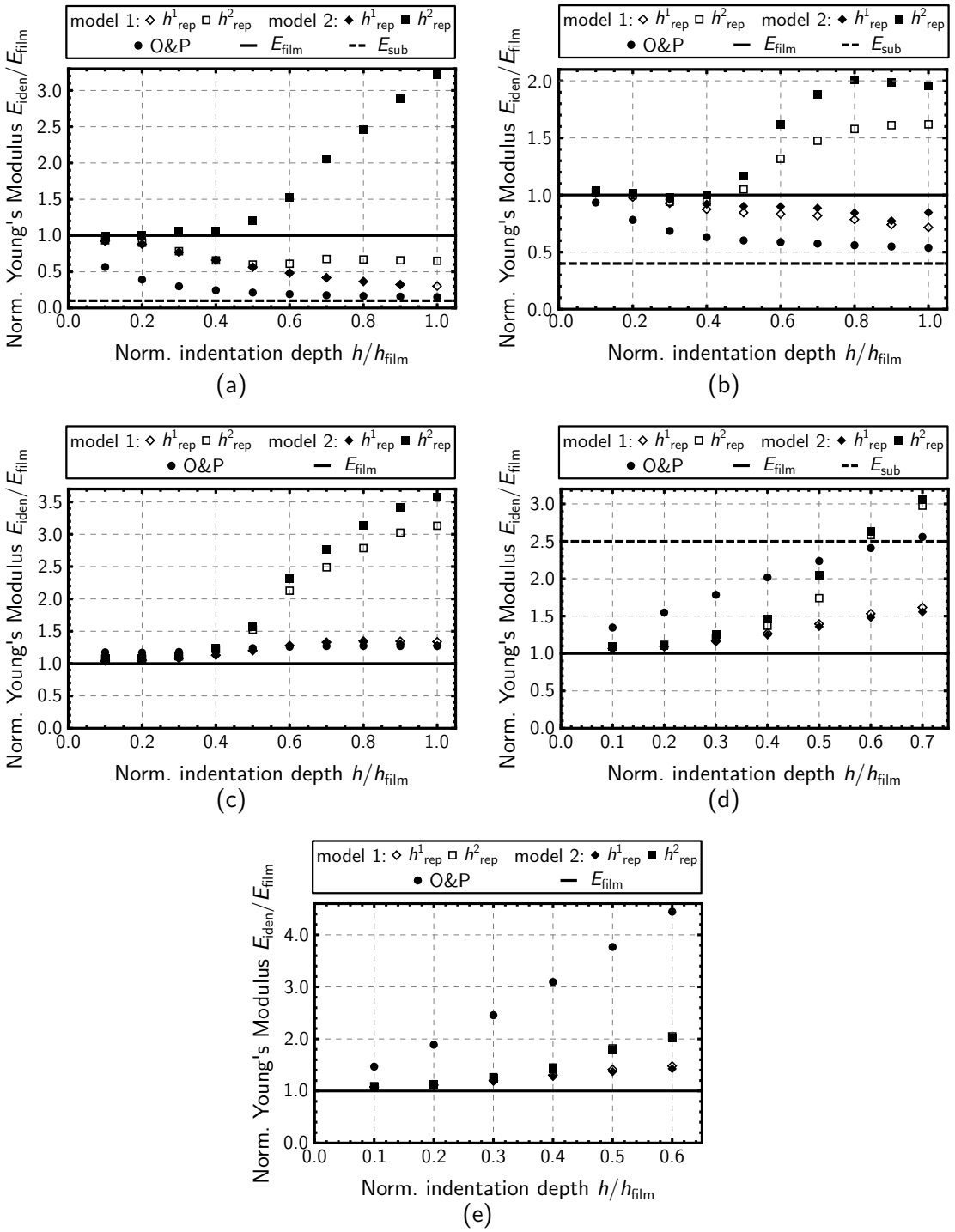

Fig. 7 Identified Young's modulus for each cone model using $h_{rep} = h^1_{rep}$ and h^2_{rep}, and contact areas evaluated from the Oliver and Pharr method. A comparison is given with estimated values from the Oliver and Pharr method denoted here by O&P. The results are presented for the following film - substrate combinations: (a) $E_{film}/E_{sub} = 10$, (b) $E_{film}/E_{sub} = 5/2$, (c) $E_{film}/E_{sub} = 1$, (d) $E_{film}/E_{sub} = 2/5$ and (e) $E_{film}/E_{sub} = 1/10$

-

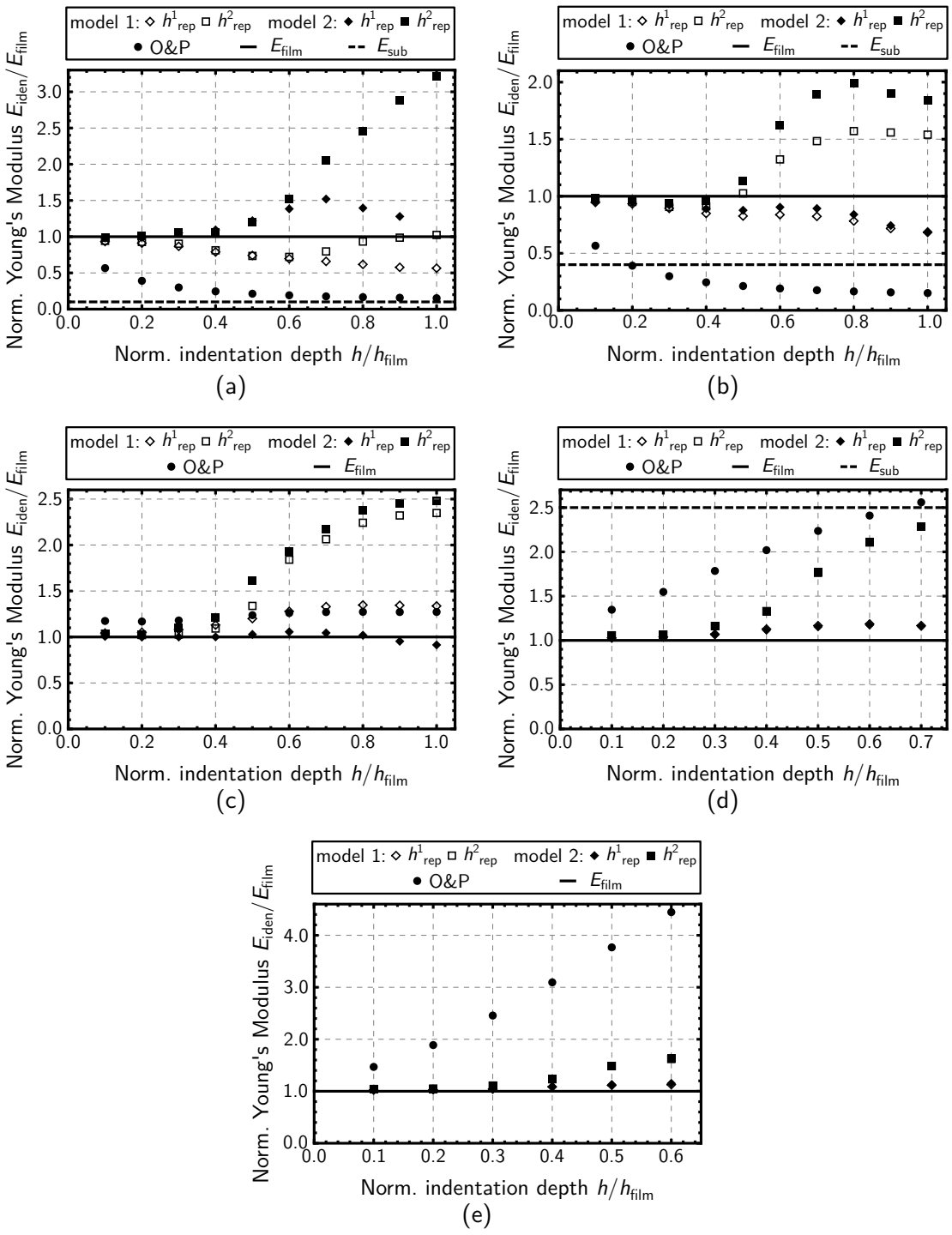

Fig. 8 Identified Young's modulus for each cone model using $h_{rep} = h^1_{rep}$ and h^2_{rep}, and contact areas evaluated from the residual imprint. A comparison is given with estimated values from Oliver and Pharr method denoted here by O&P. The results are presented for the following film - substrate combinations: (a) $E_{film}/E_{sub} = 10$, (b) $E_{film}/E_{sub} = 5/2$, (c) $E_{film}/E_{sub} = 1$, (d) $E_{film}/E_{sub} = 2/5$ and (e) $E_{film}/E_{sub} = 1/10$

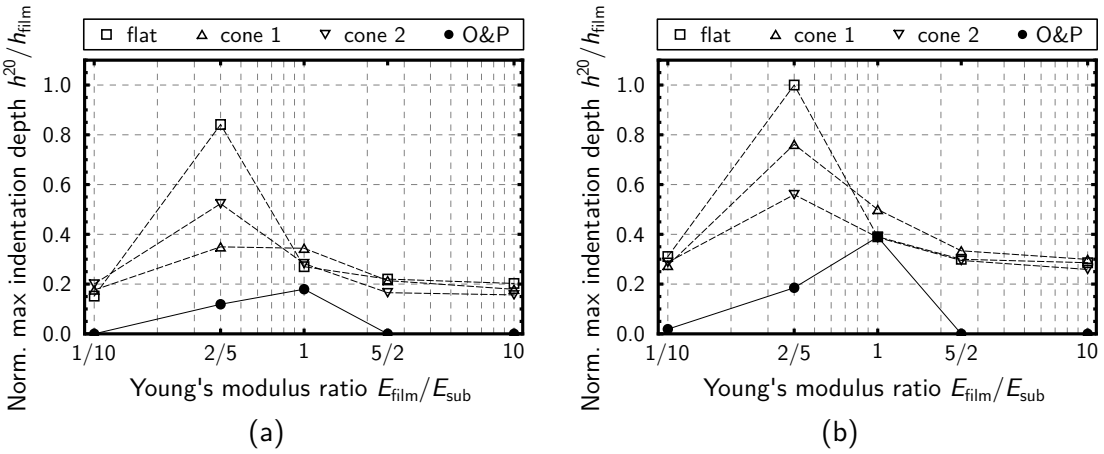

Fig. 9 Interpolated maximum indentation depth as a function of Young's modulus ratio E_{film}/E_{sub} that gives the following accuracy: (a) 10% and (b) 20%. The comparison is given between the Oliver and Pharr and proposed methods for the flat punch model, cone model 1 and cone model 2, denoted respectively O&P, flat, cone 1 and cone 2. In these results, representative thickness $h^1_{rep} = h_{film}$ and contact areas estimated from the Oliver and Pharr method were used.

5 CONCLUSIONS

This paper presented procedures using inverse analysis of the indentation contact stiffness and finite element simulation for thin films Young's modulus identification . The proposed method extend the techniques proposed in Oliver and Pharr and in Li and Vlassak and can take into account several advantages of the finite element computations for indentation problems: (i) large displacements (ii) nonlinearities (iii) Young's modulus distribution. Moreover, by further approximations, we can quickly compute the contact stiffness needed in the identification process by using simplified geometries in the finite element model.

These methods were checked against numerical examples for several film and substrate Young's moduli ratios and showed better accuracy than with Oliver and Pharr method. Nevertheless, for large indentation depths the rough simplified geometries and representative thickness lead to relatively inaccurate identified values. Therefore, further numerical investigations of the deformations during indentation of elastic-plastic layered materials should be considered to refine the simplified geometries, the representative thickness and the contact area estimation to improve the results at deep indentation depths.

ACKNOWLEDGEMENTS

J. Prou would is grateful to the Japanese Ministry of Education, Culture, Sports, Science and Technology for its financial support during his studies at Tokyo Institute of Technology.

REFERENCES

1) W. C. Oliver, G. M. Pharr, An improved technique for determining hardness and elastic modulus using load and displacement sensing indentation experiments, *J. Mater. Res.*, 7 (6) (1992), pp. 1564–1583.

2) H. Li, J. J. Vlassak, Determining the elastic modulus and hardness of an ultra-thin film on a substrate using nanoindentation, *J. Mater. Res.*, 24 (3) (2009), pp. 664–676.

3) H. Y. Yu, S. C. Sanday, B. B. Rath, The effect of substrate on the elastic properties of films determined by the indentation test – axisymmetric Boussinesq problem, 38 (6) (1990), pp. 745–764,

4) I. N. Sneddon, The relation between load and penetration in the axisymmetric Boussinesq problem for a punch of arbitrary profile, *Int. J. Eng. Sci.*, 3 (1) (1965), pp. 47–57.

5) J. Loubet, J. Georges, O. Marchesini, G. Meille, Vicker's indentation curves of magnesium oxide (MgO), *J. Tribology*, 106 (1) (1984), pp. 43–48.

6) G. Pharr, Measurement of mechanical properties by ultra low load indentation, *Mat. Sci. and Eng.: A* 253 (1998), pp. 151–159.

7) J. He, S. Veprek, Finite element modeling of indentation into superhard coatings, *Surface and Coatings Technology*, 163-164 (30) (2003) pp. 374–379.

8) F. Richter *et al*, Substrate influence in Young's modulus determination of thin films by indentation methods: Cubic boron nitride as an example, *Surface and Coatings Technology*, 201 (6) (2006), pp. 3577–3587.

9) J. Prou, K. Kishimoto, A. Constantinescu, Identification of Young's modulus from indentation testing and inverse analysis, *Journal of Solid Mechanics and Materials Engineering*, 4 (6) (2010), pp. 781–795.

10) Cast3m Finite Element Code webpage, available from http://www-cast3m.cea.fr/